Quantitative Optimization Dynamic Quantizer Design Using

Mrs.Lavanya Gullani, Mr.MD.Giasuddin , Mrs.M.Kavitha
Assistant Professor, Associate Professor , Professor
1,2,3 Department of H&S
1,2,3 Global Institute of Engineering and Technology,Moinabad,RR District, Telangana State

Abstract

Quantizers are used in networked control systems to compress continuous-valued signals into discrete-valued signals, which are subsequently sent over and received through communication channels. A quantizer must be constructed to minimize the output difference between before and after the quantizer is inserted because such quantization frequently reduces the control performance. We take into consideration the design problem for continuous-time quantizers in terms of the broad anodization and robustness of networked control systems. This work focuses on a numerical optimization approach for a continuous-time dynamic quantizer taking switching speed into account. We explain that both the temporal and spatial resolution limits can be taken into account in analysis and synthesis at the same time using a matrix uncertainty approach of sampled-data control. Finally, using numerical examples, we contrast the proposed and current strategies for sluggish switching. From

Introduction

With the rapid network technology development, the networked control systems (NCSs) have been widely studied [1–10]. One of the challenges in NCSs is quantized control. In NCSs, the continuous-valued signals are compressed and quantized to the discrete-valued signals via the quantizer of the communication channel, and such quantization often degrades the control performance. Hence, a desirable Quantier minimizes the performance error between before and after the quantizer insertion. Motivated by this, researchers [11–14] have provided optimal dynamic quantizers for the following problem foremulation in the discrete-time domain. For a given plant P, synthesize a "dynamic" quantizer Qd such that the system ΣQ composed of P and Qd in Figure 1(a) "optimally" approximates the plant P in Figure 1(b) in the sense of the input-output relation. The obtained quantizer allows us to design various controllers for the plant P on the basis of the conventional control theories. Also, this framework is helpful in not only the NCS problem but also various control problems such as hybrid control, embedded system control, and on-off actuator control. When we consider controlling a mechanical system with an on-off actuator, first the controlled object and its uncertainties are usually modelled in the continuoustime domain. Second,

the model and its uncertainties are discretized to apply the above dynamic quantizer. However, the discretization sometimes results in uncertainties more complicated than those in the original model and creates undesirable complexity in robust control. The continuoustime setting quantizer is more suitable for the robust control of the quantized system than discrete-time one. Thus, our previous works [15, 16] have considered the continuous-time setting, while a number of the discrete-time settings have been studied by others [11–14]. In these works, it is assumed that the switching process of discretizing the continuousvalued signal is sufficiently quick relative to the control frequency and only the spatial determination (quantized accuracy) is considered as the quantization effect. This is

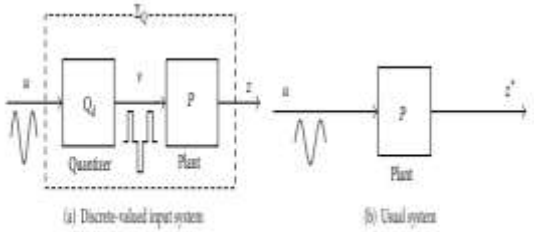

because the switching speed of the continuous-time deltasigma modulator for wireless broadband network systems is from 1 MHz to 100 MHz [17, 18]. On the other hand, the above assumption is essentially weak in the case of the slow switching such as the mechanical systems with on-off actuators [19]. For the slow switching, we need to consider the quantization effect on both the switching speed and the spatial constraints in continuous time. For example, Ishikawa et al. proposed a two-step design of a feedback modulator [20]: (I) the control performance of the modulator is considered under only the spatial

constraint, and (ii) the modulator is tuned in terms of the switching speed constraint. However, the structure of the modulator is more restricted than that of the dynamic quantizer and the obtained modulator is not always optimal. Therefore, the dynamic quantizer under temporal resolution (switching speed) and spatial resolution constraints has still to be optimally designed. The simultaneous consideration of the two constraints is the particular challenge we address in this paper. We propose a numerical optimization method for the continuous-time dynamic quantizer under switching speed and quantized accuracy constraints. To achieve the method, this paper solves the design problem via sampled-data control framework that has so far provided various results for networked control problems [7–9]. We refer to the previous work on optimal dynamic quantizer design [11, 12] and consider the basic feedforward system in Figure 1(a). In addition to the invariant set analysis [21, 22] similarly to our previous works [13, 15, 16], this paper utilizes a matrix uncertainty approach [23, 24] that is proposed in a sampleddata control framework. Although the obtained results can be more conservative than those in the previous works on continuous-time dynamic quantizer [15, 16] from the viewpoint of the class of the exogenous input and the applicable plants, both temporal and spatial resolution constraints can be addressed in analysis and synthesis, simultaneously. For the fast-switching case, the proposed conditions converge to the corresponding conditions of our previous works. Finally, for the slow switching, we compare the proposed and existing methods [15, 16] through numerical examples. In particular, a new insight is presented for the two-step design of the existing continuous-time optimal quantizer. Notation. The set of $n\times m$ (positive) real matrices is denoted by R$n\times m$ (R$n\times m$ +). The set of $n\times m$ (positive) integer matrices is denoted by N$n\times m$ (N$n\times m$ +). We denote by Lp ∞ the set

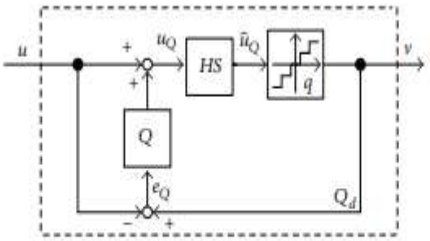

FIGURE 2: Continuous-time dynamic quantizer with switching speed h.

of piecewise-continuous functions of p-dimensional finite vectors such that ∞-norm of its functions is finite. 0$n\times m$ and Im (or for simplicity of notation, 0 and I) denote the $n\times m$ zero matrix and the $m\times m$ identity matrix, respectively. For a matrix M, MT, $\rho(M)$ and σmax(M) denote its transpose, its spectrum radius, and its maximum singular value, respectively. For a vector x, xi is the ith entry of x. For a symmetric matrix X, $X > 0$ ($X \geq 0$) means that X is positive (semi) definite. For a vector x and a sequence of vectors X: = {$x1$, $x2$, . . .}, $\|x\|$ and $\|X\|$ denote their ∞-norms, respectively. Finally, we use the "packed" notation (A B C D): = C ($sI - A$) −1B+D

Problem Formulation

Consider the discrete-valued input system ΣQ in Figure 1(a), which consists of the linear time invariant (LTI) continuoustime plant P and the quantizer V = $Qd(u)$. The system P is given by

$$P: \begin{bmatrix} \dot{x} \\ z \end{bmatrix} = \begin{bmatrix} A & B \\ C & 0 \end{bmatrix} \begin{bmatrix} x \\ v \end{bmatrix},$$

where x ∈ Rn, z ∈ Rq, u ∈ Rm, and V ∈ Rm denote the state vector, the measured output, the exogenous input, and the quantizer output, respectively. The continuous-valued signal u is quantized into the discrete-valued signal V via the quantizer Qd. We assume that the matrix A is Hurwitz; that is, the usual system in Figure 1(b) is stable in the continuoustime domain. The initial state is given as x (0) = x0. For the system P, consider the continuous-time dynamic quantizer V = $Qd(u)$ with the state vector xQ ∈ RnQ as shown in Figure 2. Its switching speed h ∈ R+ (or its temporal resolution) is determined by the operator HS, which converts

the continuous-time signal g into the low temporal resolution signal $\hat{g}$ as follows:

$$\begin{aligned} &HS: g \longrightarrow \hat{g}: \hat{g}(kh+\theta) = g[k], \\ &g[k] = g(kh), \quad k = 0,1,2,3,\ldots, \ \theta \in [0,h). \end{aligned} \tag{2}$$

That is, $\hat{uQ} = HSuQ$. S is the ideal sampler with the sampling period h and H is the zero-order hold operator. The spatial resolution of the quantizer Qd is expressed by the static quantizer q: Rm → dNm with the quantization interval d ∈ R+, that is

$$v = q(HSu_Q), \qquad u_Q = u + v_Q \tag{3}$$

and the continuous-time LTI filter Q is given by

$$\begin{bmatrix} \dot{x}_Q \\ v_Q \end{bmatrix} = \begin{bmatrix} A_Q & B_Q \\ C_Q & 0 \end{bmatrix} \begin{bmatrix} x_Q \\ e_Q \end{bmatrix}, \qquad e_Q := v - u. \tag{4}$$

Note that q is of the nearest-neighbour type toward −∞ such as the midtread quantizer in Figure 3 ($\|qi(\hat{uQi}) - \hat{uQi}\| \leq d/2$ where qi and $\hat{uQi}$ are the ith row of q and $\hat{uQ}$) and the initial state is given by xQ (0) = 0 for the drift free of Qd [11, 12]. Remark 1. In synthesis, our previous works [15, 16] ignored

the operator HS. In implementation, however, the continuous-time quantizer needs the switching process discretizing the continuous-valued signal. Of course, the applicable interval of switching depends on controlled objects such as narrowband or broadband networked systems and mechanical systems with on-off actuators. Therefore, it is important to consider the operator HS in synthesis. For the system ΣQ in Figure 1(a) with the initial state $x0$ and the exogenous input $u \in Lm\ \infty$, z (t, $x0$, $Qd(u)$) denotes the output of z at the time t. Also, for the system in Figure 1(b) without Qd, $z*$ (t, $x0$, u) denotes its output at the time t. Consider the following cost function:

$$J(Q_d) := \sup_{(x_0,u)\in\mathbb{R}^n\times\mathcal{L}^m_\infty} \sup_{t\in\mathbb{R}_+\cup\{0\}} \left\| z(t,x_0,Q_d(u)) - z^*(t,x_0,u) \right\|.$$

If the quantizer minimizes $J(Qd)$, the system ΣQ "Optimolly" approximates the usual system P in the sense of the input-output relation. In this case, we can use the existing continuous-time controller design methods for the system in Figure 1(b) without considering the quantization effect. When the controlled object and its uncertainties are modelled in the continuous-time domain, therefore, the continuous-time quantizer can introduce robust control of the continuous-time setting directly, while the discrete-time quantizer requires discretization of the whole control system. Our previous works [15, 16] proposed an optimal dynamic quantizer for the cost function $J(Qd)$ for the fast-switching case h=0. That is, only the spatial deterioration has been considered

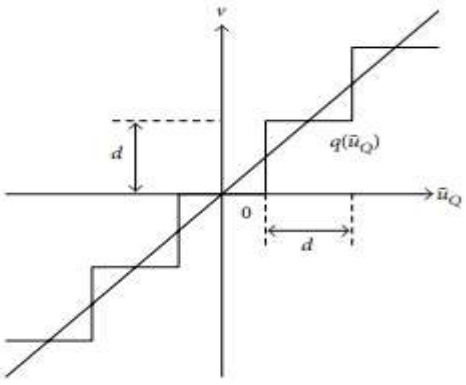

FIGURE 3: Midtread quantization.

On the other hand, the simultaneous consideration of the temporal and spatial resolution constraints is the problem we address in this paper. To consider the temporal resolution constraint caused by the operator HS, this paper modifies the cost function as follows:

$$J_{HS}(Q_d) := \sup_{(x_0,u)\in\mathbb{R}^n\times\mathcal{L}^m_\infty} \sup_{\theta\in[0,h)} \sup_{k\in\mathbb{N}_+\cup\{0\}} \left\| z(kh+\theta,x_0,Q_d(u)) - z^*(kh+\theta,x_0,u) \right\|. \quad (6)$$

Fixing θ=0 ignores the output error between before and after the quantizer is inserted over the kth sampling interval and leads to the cost function setting that is utilized for the discrete-time optimal dynamic quantizers [11–14]. Therefore, the optimal quantizer for $JHS(Qd)$ minimizes the output error between the systems in Figures 1(a) and 1(b) in terms of the input-output relation under the temporal and spatial resolution constraints. Motivated by the above, our objective is to solve the foollowing continuous-time dynamic quantizer synthesis probelm (E): for the system ΣQ composed of P and Qd with the initial state $x0 \in Rn$ and the exogenous input $u \in \ell m\ \infty$, suppose that the quantization interval $d \in R+$, the switching speed $h \in R+$, and the performance level $\gamma \in R+$ are given. Characterize a continuous-time dynamic quantizer Qd (i.e., find parameters (nQ, AQ, BQ, CQ)) achieving $JHS(Qd) \leq \gamma$. This paper proposes continuous-time quantizers in terms of solving the problem (E) on the basis of invariant set analysis and the sampled-data control technique, while other researchers [11, 12, 14] have proposed the discrete-time Optimal ones. Remark 2. The cost function setting of this paper is more complicated than the existing continuous-time and discretetime cases [11–16], so this paper considers the basic feed forward system composed of P and Qd similar to the previous works on optimal dynamic quantizer design [11, 12]. 4 Mathematical Problems in Engineering Remark 3. The plant P is restricted to be stable because of the feedforward structure, while the existing results can address unstable plants. To remove this restriction, we need to consider a feedback system structure similar to existing ones [13–16]. This is our future task.

Main Result

3.1. System Expression. In this subsection, we consider the system expression for the quantizer analysis. Define the quantization error e as

$$e := q(\hat{u}_Q) - \hat{u}_Q = v - \hat{u}_Q. \tag{7}$$

From the properties of the quantizer q and the operator HS,

$$e(kh+\theta) = e[k] \in \left[-\frac{d}{2}, \frac{d}{2}\right]^m, \quad k = 0,1,2,\ldots,\ \theta \in [0,h), \tag{8}$$

holds where $e[k] = e(kh)$. Then, one obtains

$$v(kh+\theta) = v_Q[k] + u[k] + e[k], \tag{9}$$

where $v_Q[k] = v_Q(kh)$ and $u[k] = u(kh)$ for $k = 0,1,2,\ldots$, $\theta \in [0,h)$. In this case, by using the sampled-data control technique, the following lemma holds.

Lemma 4. *Denote by $\hat{x}$ the state vector of the usual system in Figure 1(b) and define the signals as follows:*

$$\xi := \left[x^T - \hat{x}^T \ x_Q^T\right]^T, \qquad z_p := z - z^*. \tag{10}$$

Lemma 4. *Denote by $\hat{x}$ the state vector of the usual system in Figure 1(b) and define the signals as follows:*

$$\xi := \left[x^T - \hat{x}^T \ x_Q^T\right]^T, \qquad z_p := z - z^*. \tag{10}$$

For the cost function $J_{HS}(Q_d)$, the difference between $z(kh+\theta, x_0, Q_d(u))$ and $z^*(kh+\theta, x_0, u)$ for $k = 0,1,2,\ldots, \theta \in [0,h)$ is given by the following system:

$$\Sigma: \begin{cases} \xi[k+1] = \mathscr{A}\xi[k] + \mathscr{B}e[k] \\ \qquad + \begin{bmatrix} \int_0^h e^{A(h-\tau)} B\tilde{u}(kh+\tau)\mathrm{d}\tau \\ \int_0^h e^{A_Q(h-\tau)} B_Q\tilde{u}(kh+\tau)\mathrm{d}\tau \end{bmatrix} \\ z_p(kh+\theta) = \mathscr{C}(\theta)\xi[k] + \mathscr{D}(\theta)e[k] \\ \qquad + C\int_0^\theta e^{A(h-\tau)} B\tilde{u}(kh+\tau)\mathrm{d}\tau, \end{cases} \tag{11}$$

where $\xi[0] = 0$, $\tilde{u}(kh+\tau) := u[k] - u(kh+\tau)$; the matrices $\mathscr{A}$, $\mathscr{B}$, $\mathscr{C}(\theta)$, and $\mathscr{D}(\theta)$ are defined as follows:

$$\mathscr{A} := \begin{bmatrix} e^{Ah} & \int_0^h e^{A\tau}\mathrm{d}\tau BC_Q \\ 0 & e^{A_Q h} + \int_0^h e^{A_Q\tau}\mathrm{d}\tau B_Q C_Q \end{bmatrix},$$

$$\mathscr{B} := \begin{bmatrix} \int_0^h e^{A\tau}\mathrm{d}\tau B \\ \int_0^h e^{A_Q\tau}\mathrm{d}\tau B_Q \end{bmatrix}, \tag{12}$$

$$\mathscr{C}(\theta) := \left[Ce^{A\theta} \ \ C\int_0^\theta e^{A\tau}\mathrm{d}\tau BC_Q\right],$$

$$\mathscr{D}(\theta) := C\int_0^\theta e^{A\tau}\mathrm{d}\tau.$$

Proof. See Appendix A. □

We focus on $\tilde{u}(kh+\tau)$ of Σ. For the operator HS and the signal $u \in \mathscr{L}_\infty^m$,

$$\lim_{h\to 0} \|[(I - HS)u](t)\| \neq 0 \tag{13}$$

holds. This implies that we cannot ignore the temporal resolution constraint on the cost function $J_{HS}(Q_d)$ even if $h \to 0$. On the other hand, low-pass prefiltering rectifies this situation [25]. In fact, for the stable LTI system F,

$$\lim_{h\to 0} \|[(I - HS)Fu](t)\| = 0,$$
$$F := \left(\left(\begin{array}{c|c} A_F & B_F \\ \hline C_F & 0 \end{array}\right)\right) \tag{14}$$

We focus on $\tilde{u}(kh+\tau)$ of Σ. For the operator HS and the signal $u \in \mathscr{L}_\infty^m$,

$$\lim_{h\to 0} \|[(I - HS)u](t)\| \neq 0 \tag{13}$$

holds. This implies that we cannot ignore the temporal resolution constraint on the cost function $J_{HS}(Q_d)$ even if $h \to 0$. On the other hand, low-pass prefiltering rectifies this situation [25]. In fact, for the stable LTI system F,

$$\lim_{h\to 0} \|[(I - HS)Fu](t)\| = 0,$$
$$F := \left(\left(\begin{array}{c|c} A_F & B_F \\ \hline C_F & 0 \end{array}\right)\right) \tag{14}$$

holds. For the evaluation of the cost function $J_{HS}(Q_d)$, then this paper utilizes

$$u = HSFr, \quad r \in \mathscr{L}_\infty^m \tag{15}$$

as the exogenous input. Note that $u \in \mathscr{L}_\infty^m$ if stable F is strictly proper and $r \in \mathscr{L}_\infty^m$. For the signal (15), $u[k] = u(kh+\theta)$ ($k = 0,1,2,\ldots, \theta \in [0,h)$) holds, so the terms of $\tilde{u}(kh+\tau)$ in (11) are eliminated. Then, Σ is rewritten as

$$\Sigma_{HS}: \begin{cases} \xi[k+1] = \mathscr{A}\xi[k] + \mathscr{B}e[k], \\ z_p(kh+\theta) = \mathscr{C}(\theta)\xi[k] + \mathscr{D}(\theta)e[k]. \end{cases} \tag{16}$$

$$\Sigma_{HS}: \begin{cases} \xi[k+1] = \mathscr{A}\xi[k] + \mathscr{B}e[k], \\ z_p(kh+\theta) = \mathscr{C}(\theta)\xi[k] + \mathscr{D}(\theta)e[k]. \end{cases}$$

Also, this paper solves the following synthesis problem (E□): for the system ΣQ composed of P and Qd with the initial state $x0 \in \mathrm{R}n$ and the exogenous input $u \in \mathrm{L}m\,\infty$ in (15), suppose that the quantization interval $d \in \mathrm{R}+$, the switching speed $h \in \mathrm{R}+$, and the performance level $\gamma \in \mathrm{R}+$ are given. Characterize a continuous-time dynamic

quantizer Qd (i.e., find parameters (nQ, AQ, BQ, CQ)) achieving $JHS(Qd)$

3.2. Quantizer Analysis. The quantization error e of (16) is bounded as mentioned earlier. The reachable set and the invariant set characterize such a system with bounded input. Consider the LTI discrete-time system given by

$$\tilde{\xi}[k+1] = \mathscr{A}\tilde{\xi}[k] + \mathscr{B}w[k],$$

$$\mathbb{R}_\infty := \left\{ \tilde{\xi} \in \mathbb{R}^{n_\xi} \;\middle|\; \begin{array}{l} \exists k \in \mathbb{N}_+ \;\; \exists w[\cdot] \in \mathbb{W}, \\ \tilde{\xi}[k] = \sum_{i=0}^{k-1} \mathscr{A}^{k-1-i}\mathscr{B}w[i] \end{array} \right\}, \quad (18)$$

$$\mathbb{W} := \left\{ w \in \mathbb{R}^m : w^T w \le 1 \right\}.$$

Definition 6. Define the invariant set of the system (17) to be a set x which satisfies

$$\tilde{\xi} \in x, \quad w \in \mathbb{W} \Longrightarrow \mathscr{A}\tilde{\xi} + \mathscr{B}w \in x. \quad (19)$$

The analysis condition can be expressed in terms of matrix inequalities as summarized in the following proposition [22].

Proposition 7. *Consider the system* (17). *For a matrix* $0 < \mathscr{P} = \mathscr{P}^T \in \mathbb{R}^{n_\xi \times n_\xi}$, *the ellipsoid* $\mathbb{E}(\mathscr{P}) := \{\tilde{\xi} \in \mathbb{R}^{n_\xi} : \tilde{\xi}^T \mathscr{P} \tilde{\xi} \le 1\}$ *is an invariant set if and only if there exists a scalar* $\alpha \in [0, 1 - \rho(\mathscr{A})^2]$ *satisfying*

$$\begin{bmatrix} \mathscr{A}^T\mathscr{P}\mathscr{A} - (1-\alpha)\mathscr{P} & \mathscr{A}^T\mathscr{P}\mathscr{B} \\ \mathscr{B}^T\mathscr{P}\mathscr{A} & \mathscr{B}^T\mathscr{P}\mathscr{B} - \alpha I_m \end{bmatrix} \le 0. \quad (20)$$

Note that the ellipsoidal set $\mathbb{E}(\mathscr{P})$ covers the reachable set $\mathbb{R}_\infty$ from outside. Define the set $\mathscr{E} := \{\tilde{w} \in \mathbb{R}^m : e = (\sqrt{md}/2)\tilde{w}$ satisfies (7)$\}$ and rewrite the system (16) as

$$\tilde{\Sigma}_{HS} : \begin{cases} \tilde{\xi}[k+1] = \mathscr{A}\tilde{\xi}[k] + \mathscr{B}\tilde{w}[k], \\ \tilde{z}_p(kh+\theta) = \mathscr{C}(\theta)\tilde{\xi}[k] + \mathscr{D}(\theta)\tilde{w}[k], \end{cases} \quad (21)$$

$$\mathbb{R}_\infty := \left\{ \tilde{\xi} \in \mathbb{R}^{n_\xi} \;\middle|\; \begin{array}{l} \exists k \in \mathbb{N}_+ \;\; \exists w[\cdot] \in \mathbb{W}, \\ \tilde{\xi}[k] = \sum_{i=0}^{k-1} \mathscr{A}^{k-1-i}\mathscr{B}w[i] \end{array} \right\}, \quad (18)$$

$$\mathbb{W} := \left\{ w \in \mathbb{R}^m : w^T w \le 1 \right\}.$$

Definition 6. Define the invariant set of the system (17) to be a set x which satisfies

$$\tilde{\xi} \in x, \quad w \in \mathbb{W} \Longrightarrow \mathscr{A}\tilde{\xi} + \mathscr{B}w \in x. \quad (19)$$

The analysis condition can be expressed in terms of matrix inequalities as summarized in the following proposition [22].

Proposition 7. *Consider the system* (17). *For a matrix* $0 < \mathscr{P} = \mathscr{P}^T \in \mathbb{R}^{n_\xi \times n_\xi}$, *the ellipsoid* $\mathbb{E}(\mathscr{P}) := \{\tilde{\xi} \in \mathbb{R}^{n_\xi} : \tilde{\xi}^T \mathscr{P} \tilde{\xi} \le 1\}$ *is an invariant set if and only if there exists a scalar* $\alpha \in [0, 1 - \rho(\mathscr{A})^2]$ *satisfying*

$$\begin{bmatrix} \mathscr{A}^T\mathscr{P}\mathscr{A} - (1-\alpha)\mathscr{P} & \mathscr{A}^T\mathscr{P}\mathscr{B} \\ \mathscr{B}^T\mathscr{P}\mathscr{A} & \mathscr{B}^T\mathscr{P}\mathscr{B} - \alpha I_m \end{bmatrix} \le 0. \quad (20)$$

Note that the ellipsoidal set $\mathbb{E}(\mathscr{P})$ covers the reachable set $\mathbb{R}_\infty$ from outside. Define the set $\mathscr{E} := \{\tilde{w} \in \mathbb{R}^m : e = (\sqrt{md}/2)\tilde{w}$ satisfies (7)$\}$ and rewrite the system (16) as

$$\tilde{\Sigma}_{HS} : \begin{cases} \tilde{\xi}[k+1] = \mathscr{A}\tilde{\xi}[k] + \mathscr{B}\tilde{w}[k], \\ \tilde{z}_p(kh+\theta) = \mathscr{C}(\theta)\tilde{\xi}[k] + \mathscr{D}(\theta)\tilde{w}[k], \end{cases} \quad (21)$$

Along with this, $\tilde{z}_p$ of (21) is also rewritten as

$$\begin{aligned} &\tilde{z}_p(kh+\theta) \\ &= \left[C + C\Omega(\theta)A \;\; C\Omega(\theta)BC_Q\right]\tilde{\xi}[k] + C\Omega(\theta)\tilde{w}[k] \\ &= \left(\widehat{\mathscr{C}} + C\Omega(\theta)\widehat{\mathscr{D}}\right)\tilde{\xi}[k] + C\Omega(\theta)\tilde{w}[k], \\ &\qquad \widehat{\mathscr{C}} := [C \;\; 0], \qquad \widehat{\mathscr{D}} := [A \;\; BC_Q]. \end{aligned} \quad (23)$$

In addition, from the properties of $\mathbb{R}_\infty$ and $\mathbb{E}(\mathscr{P})$,

$$\begin{aligned} &J_{HS}(Q_d) \\ &\le \sup_{\theta\in[0,h)} \sup_{\tilde{\xi}\in\mathbb{R}_\infty, \tilde{w}\in\mathscr{E}} \left\|\mathscr{C}(\theta)\tilde{\xi} + \mathscr{D}(\theta)\tilde{w}\right\| \frac{\sqrt{md}}{2} \\ &\le \sup_{\theta\in[0,h)} \sup_{\tilde{\xi}\in\mathbb{R}_\infty, \tilde{w}\in\mathbb{W}} \left\|\mathscr{C}(\theta)\tilde{\xi} + \mathscr{D}(\theta)\tilde{w}\right\| \frac{\sqrt{md}}{2} \quad (\because \mathscr{E} \subseteq \mathbb{W}) \\ &\le \sup_{\theta\in[0,h)} \sup_{\tilde{\xi}\in\mathbb{E}(\mathscr{P}), \tilde{w}\in\mathbb{W}} \left\|\mathscr{C}(\theta)\tilde{\xi} + \mathscr{D}(\theta)\tilde{w}\right\| \frac{\sqrt{md}}{2} \\ &\qquad\qquad (\because \mathbb{R}_\infty \subseteq \mathbb{E}(\mathscr{P})) \\ &\le \underbrace{\sup_{\theta\in[0,h)} \sup_{\tilde{\xi}\in\mathbb{E}(\mathscr{P})} \left\|\left(\widehat{\mathscr{C}} + C\Omega(\theta)\widehat{\mathscr{D}}\right)\tilde{\xi}\right\| \frac{\sqrt{md}}{2}}_{\gamma_1} \\ &\quad + \underbrace{\sup_{\theta\in[0,h)} \sup_{\tilde{w}\in\mathbb{W}} \left\|C\Omega(\theta)\tilde{w}\right\| \frac{\sqrt{md}}{2}}_{\gamma_2} \end{aligned} \quad (24)$$

holds. Similarly to our previous papers [13, 15, 16], by using the L1 control technique in [21], we provide the sufficient conditions for computing $\gamma 1 \in \mathrm{R}+$ and $\gamma 2 \in \mathrm{R}+$ of (24) as follows:

$$\begin{bmatrix} \mathcal{P} & \widehat{\mathscr{C}}^T + \widehat{\mathscr{D}}^T \Omega(\theta)^T C^T \\ \widehat{\mathscr{C}} + C\Omega(\theta)\widehat{\mathscr{D}} & \gamma_1^2 I_q \end{bmatrix} \geq 0, \qquad (25)$$
$$\Omega(\theta)^T C^T C \Omega(\theta) \leq \gamma_2^2 I_n, \quad \forall \theta \in [0,h).$$

Remark 8. For the inequalities (25) and any vectors $\tilde{\xi} \in \mathbb{R}^n$ and $\tilde{w} \in \mathbb{R}^m$, we have

$$\begin{bmatrix} \tilde{\xi}^T \mathcal{P} \tilde{\xi} & \tilde{\xi}^T \left(\widehat{\mathscr{C}}^T + \widehat{\mathscr{D}}^T \Omega(\theta)^T C^T\right) \\ \left(\widehat{\mathscr{C}} + C\Omega(\theta)\widehat{\mathscr{D}}\right)\tilde{\xi} & \gamma_1^2 I_q \end{bmatrix} \geq 0$$
$$\Longleftrightarrow \tilde{\xi}^T \left(\widehat{\mathscr{C}} + C\Omega(\theta)\widehat{\mathscr{D}}\right)^T \left(\widehat{\mathscr{C}} + C\Omega(\theta)\widehat{\mathscr{D}}\right)\tilde{\xi} \qquad (26)$$
$$\leq \gamma_1^2 \tilde{\xi}^T \mathcal{P} \tilde{\xi} \quad (\because \text{Schur complement})$$

and $\tilde{w}^T \Omega(\theta)^T C^T C \Omega(\theta) \tilde{w} \leq \gamma_2^2 \tilde{w}^T \tilde{w}$. Then, we see that (24) holds if $\tilde{\xi} \in \mathbb{E}(\mathcal{P})$ and $\tilde{w} \in \mathbb{W}$.

The inequalities (25) are difficult to test since we need to find P, $\gamma 1$, and $\gamma 2$ satisfying (20) and (25) for infinitely many values of $\theta \in [0, h)$. Then, using the matrix uncertainty technique [23, 24], we consider their sufficient conditions, which are easy to compute. Considering $\Omega(\theta)$ in (22) as a matrix uncertainty, we introduce the following lemma regarding the matrix exponential [26, 27]

Lemma 9. *For the matrix $\Omega(\theta)$ in (22),*

$$\sigma_{\max}(\Omega(\theta)) \leq \delta(\theta) \leq \delta(h), \quad \forall \theta \in [0,h), \qquad (27)$$

holds where

$$\delta(\theta) := \begin{cases} \dfrac{e^{\mu(A)\theta} - 1}{\mu(A)}, & \mu(A) \neq 0, \\ \theta, & \mu(A) = 0, \end{cases} \qquad (28)$$
$$\mu(A) := \max\left\{\lambda : \lambda \in eig\left(\frac{A + A^T}{2}\right)\right\}.$$

Proof. Since $\sigma_{\max}(e^{A\theta}) \leq e^{\mu(A)\theta}$ (see [26]),

$$\sigma_{\max}(\Omega(\theta)) \leq \int_0^\theta \sigma_{\max}\left(e^{A\beta}\right) d\beta \leq \int_0^\theta e^{\mu(A)\beta} d\beta \qquad (29)$$

holds. □

By using Lemma 9 and the S-procedure [23, 28, 29], the sufficient condition analysing the cost function $JHS(Qd)$ of the system ΣQ can be expressed in terms of matrix inequality as summarized in the following theorem. Theorem 10. Consider the system ΣQ composed of P and Qd with the initial state $x0 \in \mathrm{R}n$ and the exogenous input $u \in \mathrm{L}m \infty$ in (15). For the quantization interval $d \in \mathrm{R}+$ and the switching speed $h \in \mathrm{R}+$, the upper bound of the cost function $JHS(Qd)$ is given by

$$\|T_{HS}(Q_d)\| \leq \gamma(h)$$
$$s.t.\ \gamma(h) := \left(\gamma + \sigma_{\max}(C)\delta(h)\right)\frac{\sqrt{m}d}{2} \qquad (30)$$

if there exist $0 < \mathbb{Q} = \mathbb{Q}^T \in \mathbb{R}^{(n+n_Q)\times(n+n_Q)}$, $0 < S = S^T \in \mathbb{R}^{n\times n}$, $\alpha_h \in [0, 1/2h - \rho(\mathscr{A})^2/2h]$ *and* $\gamma \in \mathbb{R}_+$ *satisfying*

$$\begin{bmatrix} \Phi_h \mathbb{Q} + \mathbb{Q}\Phi_h^T + 2\alpha_h \mathbb{Q} & \Gamma_h & \sqrt{h}\mathbb{Q}\Phi_h^T \\ \Gamma_h^T & -2\alpha_h I_m & \sqrt{h}\Gamma_h^T \\ \sqrt{h}\Phi_h \mathbb{Q} & \sqrt{h}\Gamma_h & -\mathbb{Q} \end{bmatrix} \leq 0, \qquad (31)$$

$$\begin{bmatrix} \mathbb{Q} & \mathbb{Q}\widehat{\mathscr{C}}^T & \sqrt{\delta(h)}\mathbb{Q}\widehat{\mathscr{D}}^T \\ \widehat{\mathscr{C}}\mathbb{Q} & \gamma^2 I_q - \delta(h) CSC^T & 0 \\ \sqrt{\delta(h)}\widehat{\mathscr{D}}\mathbb{Q} & 0 & S \end{bmatrix} \geq 0, \qquad (32)$$
$$S\Omega(\theta) = \Omega(\theta) S, \quad \forall \theta \in [0,h),$$

where the matrices Φ_h *and* Γ_h *are defined by*

$$\Phi_h := \begin{bmatrix} \frac{1}{h}\int_0^h e^{A\tau} d\tau A & \frac{1}{h}\int_0^h e^{A\tau} d\tau B C_Q \\ 0 & \frac{1}{h}\int_0^h e^{A_Q \tau} d\tau \left(A_Q + B_Q C_Q\right) \end{bmatrix}, \qquad (33)$$

$$\Gamma_h := \begin{bmatrix} \frac{1}{h}\int_0^h e^{A\tau} d\tau B \\ \frac{1}{h}\int_0^h e^{A_Q \tau} d\tau B_Q \end{bmatrix}.$$

Proof. See Appendix A. □

Denote by $\hat{\Sigma}$ the system Σ without operator HS. In this case, the system $\hat{\Sigma}$ is given by

$$\hat{\Sigma} : \dot{\xi}(t) = \widehat{\mathscr{A}}\xi(t) + \widehat{\mathscr{B}}e(t), \qquad z_p(t) = \widehat{\mathscr{C}}\xi(t), \qquad (34)$$

where

$$\widehat{\mathscr{A}} := \begin{bmatrix} A & BC_Q \\ 0 & A_Q + B_Q C_Q \end{bmatrix}, \qquad \widehat{\mathscr{B}} := \begin{bmatrix} B \\ B_Q \end{bmatrix}. \qquad (35)$$

Regarding the definition of $\xi(t)$, see Lemma 4. An advantage the condition (31) over conditions (20) is that it can be used for a small h without numerical difficulty. This idea comes from [23, 24]. In the limit of $h \to 0$, $(1/h) \int h\ 0\ e\ A$and$\tau \to I$ and $(1/h) \int h\ 0\ e\ AQh\ d\tau \to I$ hold, so $\Phi h \to \hat{\mathrm{A}}$ and $\Gamma h \to \hat{\mathrm{B}}$ hold. In the same limit, from $\delta(h) \to 0$, conditions (31) and (32) converge to the analysis conditions of the

continuoustime dynamic quantizer for the system Σ in [15, 16]. On the other hand, for a small h, $e\ Ah \to I$, $e\ AQh \to I$, $\int h\ 0\ e\ A$dοτ→0 and $\int h\ 0\ e\ AQh$ dτ→0 hold, so A and B (A and B) are close to identity and zero matrices, respectively, and the left side of (20) is close to zero. In numerical computation, it is appropriate to fix the structure of S such that $S\Omega(\theta) = \Omega(\theta)S$ holds. For example, we can set $S=s\theta In$, $s\theta \in$ R+ and this setting leads to the

(i) *There exist matrices* $0 < \mathcal{Q} = \mathcal{Q}^T \in \mathbb{R}^{(n+n_Q)\times(n+n_Q)}$, $0 < S = S^T \in \mathbb{R}^{n\times n}$ *and a dynamic quantizer* Q_d *satisfying* (31), (32), *and* (38).

(ii) *There exist matrices* $0 < Y = Y^T \in \mathbb{R}^{n\times n}$, $0 < V = V^T \in \mathbb{R}^{n\times n}$, $W \in \mathbb{R}^{m\times n}$, $0 < S = S^T \in \mathbb{R}^{n\times n}$ *satisfying*

$$\begin{bmatrix} \Theta_{Ah} + \Theta_{Ah}^T + 2\alpha_h\Theta_P & \Theta_{Bh} & \sqrt{h}\Theta_{Ah}^T \\ \Theta_{Bh}^T & -2\alpha_h I_m & \sqrt{h}\Theta_{Bh}^T \\ \sqrt{h}\Theta_{Ah} & \sqrt{h}\Theta_{Bh} & -\Theta_P \end{bmatrix} \le 0, \quad (40)$$

$$\begin{bmatrix} \Theta_P & \Theta_C^T & \Theta_{Dh}^T \\ \Theta_C & \gamma^2 I_q - \delta(h)\, CSC^T & 0 \\ \Theta_{Dh} & 0 & S \end{bmatrix} \ge 0, \quad (41)$$

$$S\Omega(\theta) = \Omega(\theta)S, \quad \forall\theta \in [0, h),$$

following optimization problem (Atop)

$$\min_{\mathcal{Q}=\mathcal{Q}^T>0, S=s_\theta I_n>0, 1/2h-\rho(\mathcal{A})^2/2h\ge\alpha_h\ge0, \gamma>0} \gamma^2 \quad (36)$$

s.t. (31) and (32).

When scalar α_h is fixed, the conditions in Theorem 10 are linear matrix inequalities (LMIs) in terms of the other variables. Using standard LMI software and the line search of α_h, we can obtain an upper bound of $J_{HS}(Q_d)$.

3.3. Quantizer Synthesis. The problem **(Aop)** suggests that the quantizer synthesis problem (E′) is reduced to the following nonconvex optimization problem **(OP)**:

$$\min_{\mathcal{Q}=\mathcal{Q}^T>0, S=s_\theta I_n>0, A_Q, B_Q, C_Q, 1/2h-\rho(\mathcal{A})^2/2h\ge\alpha_h\ge0, \gamma>0} \gamma^2 \quad (37)$$

s.t. (31) and (32).

That is, if **(OP)** is feasible, (E′) is feasible.

From the matrix product such as $(1/h)\ \int h\ 0\ e\ AQh$ dτ and $AQ+BQCQ$ in (31), the synthesis condition is difficult to derive from Theorem 10 unlike the continuous-time case without the operator HS in [15, 16]. Thus, we fixed the parameters as follows:

$$n_Q = n, \qquad A_Q = A, \qquad B_Q = B. \quad (38)$$

The structure (38) does not severely limit the synthesis because AQ and BQ of the continuous-time dynamic quanttiger for the system Σ in [15, 16] are also (38). See Appendix B. In other words, $xQ = AxQ + BeQ$ estimates the quantization influence on the system P. Along with this, we fix Q of (31) as follows:

$$\mathcal{Q} = \begin{bmatrix} Y & V \\ V & V \end{bmatrix}, \quad Y = Y^T > 0, \quad V = V^T > 0. \quad (39)$$

The structure (39) also does not impose a severe limitation on the synthesis because an appropriate choice of the quantizer state coordinates allows us to assume that Q has the special structure for the full order case $nQ = n$ [30]. Under some circumstances (38) and (39), we obtain the following synthesis condition. Theorem 11. Consider the system ΣQ composed of P and Qd with the initial state $x0 \in$ Rn and the exogenous input $u \in$ L$m\ \infty$ in (15). Suppose that the quantization interval $d \in$ R+, the switching speed $h \in$ R+, and the performance level $\gamma \in$ R+ are given. For a scalar $\alpha h \in [0, 1/2h]$, there exist a continuous-time dynamic quantizer Qd achieving (30) if one of the following equivalent statements holds.

where

$$\Theta_P := \begin{bmatrix} Y & V \\ V & V \end{bmatrix}, \qquad \Psi_h := \frac{1}{h}\int_0^h e^{A\tau} d\tau,$$

$$\Theta_{Ah} := \begin{bmatrix} \Psi_h(AY + BW) & \Psi_h(AV + BW) \\ \Psi_h(AV + BW) & \Psi_h(AV + BW) \end{bmatrix},$$

$$\Theta_{Bh} := \begin{bmatrix} \Psi_h B \\ \Psi_h B \end{bmatrix}, \qquad \Theta_C := [CY \ \ CV],$$

$$\Theta_{Dh} := \left[\sqrt{\delta(h)}(AY + BW) \ \ \sqrt{\delta(h)}(AV + BW)\right]. \quad (42)$$

In this case, such a quantizer parameter is given by

$$n_Q = n, \qquad A_Q = A, \qquad B_Q = B, \qquad C_Q = WY^{-1}. \quad (43)$$

Proof. We fix Q as shown in (39) and introduce the change of variables $W=CQY$. Hence, (31) and (32) result in (40) and (41). Also, designing CQ yields $\alpha h \in [0, 1/2h]$ because ρ(A) is determined by CQ and $[0, 1/2h - \rho(A)\ 2\ /2h] \subseteq [0, 1/2h]$. In the limit of h→0; Ψh converges to I and $\delta(h)$ converges to 0; then conditions (40) and (41) also converge to the synthesis condition of the continuous-time dynamic quantizer for the system Σ in (34). Also, by setting $S=s\theta In$ for Theorem 11, the quantizer synthesis problem (E□) is reduced to the following optimization problem (Sop)

$$\min_{Y=Y>0^T, V=V^T>0, S=s_g I_n>0, W, 1/2h\geq\alpha_h\geq 0, \gamma>0} \gamma^2 \quad (44)$$

s.t. (40) and (41).

If (Sop) is feasible, (E□) is feasible. Therefore, a continuoustime dynamic quantizer considering both spatial and temporeal resolution constraints is obtained from Theorem 11. Remark 12. To consider numerical optimization analysis or synthesis of a quantizer as shown in (Atop) and (Sop), we need the signal assumption (15) in Theorems 10 and 11. On the other hand, for the high-speed switching such that h is very small, the assumption (15) ensures that solutions to the problem (E□) converge to us

previous results [15, 16]. Therefore, the results of this paper partly include our previous results [15, 16] although each class of exogenous signals and plants is restricted

Discussion

For the slow switching, we compare the proposed method and existing continuous-time quantizer [15, 16]. Consider the system ΣQ. The plant P is the stable minimum phase LTI system:

$$\begin{bmatrix} \dot{x}(t) \\ z(t) \end{bmatrix} = \begin{bmatrix} -3 & 3 & 0 \\ 0 & -2 & 2 \\ 1 & 1 & 0 \end{bmatrix} \begin{bmatrix} x(t) \\ v(t) \end{bmatrix}. \quad (45)$$

In the case without the operator HS, an optimal form of the continuous-time quantizer $Qop\ d$ [15, 16] is given by (B.2)

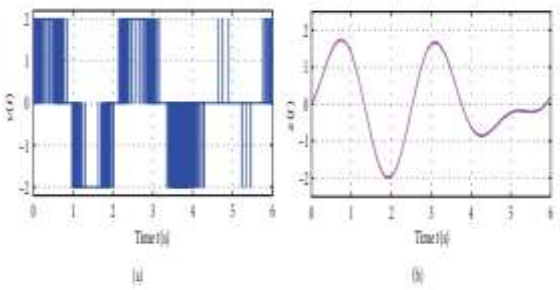

Figure 4: Time responses of ΣQ with the proposed quantizer for $h = 0.01$

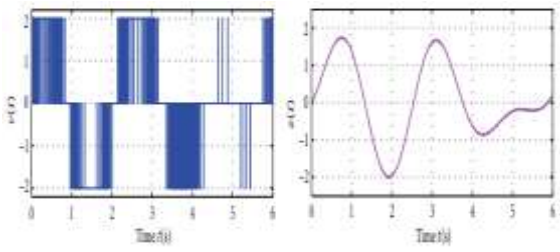

Figure 5: Time responses of ΣQ with (B.2) for $h = 0.01$.

See Appendix B. The continuous-time quantizer $Qop\ d$ and its performance are parameterized by the free parameter $f \in$ R+. For the simulation, we consider a two-step design for $Qop\ d$; we first set f and second insert the operator HS in the obtained $Qop\ d$. Also, the achievable performance of JHS $(Qop\ \ d)$ is calculated by (Atop). For the comparison, we set the switching speed $h = 0.01$ [s] and the quantization interval d=2. First, we set f = 50 and then obtain $Qop\ d$ with $\gamma c = 0.102$. Also, $\gamma(h) = 0.219$ for JHS $(Qop\ d)$ is obtained from (Atop). Second, we solve the problem (Sop) and obtain $\gamma(h) = 0.219$ and the matrix CQ = [−19.26 −22.72]. In this case, both quantizers can approximate well. Figures 4 and 5 illustrate the simulation results of the time responses of ΣQ with the proposed quantizer and the quantizers $Qop\ d$ in (B.2). The initial state $x0$ = [0 0] T and the input $u(t)$ = sin πt + cos $0.7\pi t$ are given. In Figures 4 and 5, the thin lines and the thick lines are for the conventional system in Figure 1(b) and the system ΣQ in Figure 1(a), respectively. We see that the controlled outputs of the discrete-valued input systems with the dynamic quantizers approximate those of the usual systems even if the quantized outputs are applied. Also, the two controlled outputs approximated by both quantizers are exactly the same. Next, we consider the case h = 0.1. In this case, the two controlled outputs approximated by the two quantizers differ. (Atop)for $Qop\ d$ is infeasible. From (Sop), on the other hand, we obtain $\gamma(h) = 0.949$ and the matrix CQ = [−1.1321 −3.097]. Figures 6 and 7 illustrate the simulation results on the time responses of ΣQ with (B.2) and the proposed quantizer in the same fashion. We see that $z(t)$ of the usual plant P is approximated by $z(t)$ of the system ΣQ with the proposed quantizer, while $z(t)$ of the system ΣQ with (B.2) diverges. From this example, we see that the proposed method can address the spatial resolution and the temporal resolution issues, simultaneously. Also, Theorem 10 verifies whether the quantizer $Qop\ d$ is applicable to the given switching speed setting. Remark 13. In the above numerical experiments, the proposed quantizer is designed and the quantizer $Qop\ d$ is analysed for u = HSF (sin πt + cos $0.7\pi t$), while the time responses of the quantizers are simulated for u = sin πt + cos $0.7\pi t$. That is, this is the conservativeness caused by the signal assumption (15). However, we see that the above results verify the effectiveness of the proposed method even if the signal conservativeness exists. Here, we focus on the eigenvalues of A for the system Σ with $Qop\ d$. The eigenvalues for f = 50 and h = 0.1 are {0.741, 0.819, 0.550, −4.21} and then A is unstable in the discrete-time domain. From Theorem 10, (Atop) is infeasible if ρ(A) is bigger than 1 (in other words, A is unstable). {0.741, 0.819} are the

eigenvalues of $e\ Ah$. That is, $e\ AQh + \int h\ 0\ e\ AQ\tau$ $d\tau BQCQ$ (=: $AQ(h)$) for $Qop\ d$ is unstable. Then, we consider the case in which f=3 and h = 0.1 (γc = 0.707) such that $AQ(h)$ is stable. The corresponding eigenvalues are {0.637, 0.354}. In this case, $\gamma(h)$ = 1.085 for JHS ($Qop\ d$) is obtained from (Atop). From the above results, the existing continuous-quantizer in [15, 16] may be suitable for a two-step design such that $AQ(h)$ is stable via the parameter f. In terms of the upper

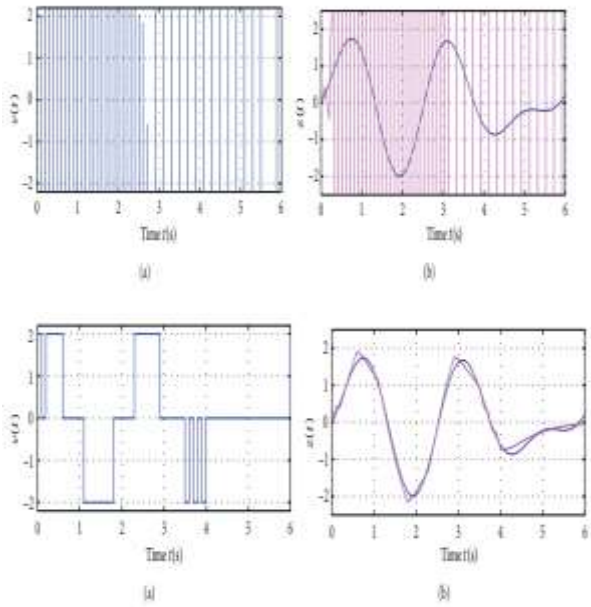

Figure 7: Time responses of ΣQ with the proposed quantizer for h = 0.1

bound of cost function (B.3), first, let us consider the problem **(P-1)**: maximize f for Q_d^{op} such that

$$\exists X^T = X > 0 \quad \text{s.t. } A_Q(h)^T X A_Q(h) - X < 0, \qquad (46)$$

where the parameters (A_Q, B_Q, C_Q) of $A_Q(h)$ are given by (B.2). This problem is LMI for the line search of f. For h = 0.1, its solution is f = 18.9 (γ_c = 0.173). However, $\gamma(h)$ = 113.148 for $J_{HS}(Q_d^{op})$ is obtained from **(Aop)**. By using Theorem 10, next, let us consider the problem **(P-2)**:

$$\min_{\Theta=\Theta^T>0, S=s_0 I_n>0, 1/2h-(\rho(\Delta f)^2)/2h\geq\alpha_h\geq 0, f>0, \gamma>0} \gamma^2 \qquad (47)$$

s.t. (31) and (32),

where the parameters (AQ, BQ, CQ) of Ψh and Γh are given by (B.2). This problem is LMI for the plane search of f and αh. For h = 0.1, its solution is f = 5.715 (γc = 0.397) and then $\gamma(h)$ = 0.949 for $JHS(Qop\ d\ )$ is obtained. This performance is about the same as that of the proposed quantizer. Therefore, we see that Theorem 10 is also helpful for the two-step design of the existing continuous-time quantizer [15, 16] even if the tractable optimization method instead of the plane search remains an issue for future work. Such a method correlates the parameter f with the switching speed h, so its insight is expected not only to result in a new two-step design but also to clarify the relationship between the discrete-time and continuous-time dynamic quantizers. Of course, important future topics also include considering the quantized feedback control system with unstable plants and generalizing the exogenous signal for the evaluation of the cost function.

Conclusion

This research has discussed continuous-time quantized control with a focus on broadbandization and robustness of networked control systems. On the basis of the invariant set analysis and the sampled-data control methodology, we have suggested numerical optimization methods for synthesizing and analyzing the continuous-time dynamic quantizer. The benefits of the suggested approach can be summed up as follows. I Unlike Ishikawa et al. [20] and us [15, 16], who previously overlooked the timing limitation in synthesis, both the temporal and spatial resolution limits can be taken into account concurrently. The proposed approach can therefore be used for both fast and slow switching scenarios. (ii) It has been demonstrated that each sample interval's highest output difference can be quantified numerically using

Appendix A. Proof:

Proof. $z(kh+\theta)$ for $k = 0, 1, 2, \ldots, \theta \in [0, h)$ (which is the behavior of $z(t)$ over the kth sampling interval) is given by the discretized system of P:

$$\begin{aligned} x[k+1] &= e^{Ah}x[k] + \int_0^h e^{A(h-\tau)}Bv(kh+\tau)\,d\tau \\ z(kh+\theta) &= Ce^{A\theta}x[k] + C\int_0^\theta e^{A(\theta-\tau)}Bv(kh+\tau)\,d\tau, \end{aligned} \tag{A.1}$$

where $x[k] = x(kh)$. $v(t)$ is given by (9) and $v_Q[k]$ is given by the discretized system of Q:

$$\begin{aligned} &x_Q[k+1] \\ &= \left(e^{A_Q h} + \int_0^h e^{A_Q\tau}d\tau B_Q C_Q\right)x_Q[k] + \int_0^h e^{A_Q\tau}d\tau B_Q e[k] \\ &\quad + \int_0^h e^{A_Q(h-\tau)}B_Q\tilde{u}(kh+\tau)\,d\tau, \\ &\qquad v_Q[k] = C_Q x_Q[k], \end{aligned} \tag{A.2}$$

where $x_Q[k] = x_Q(kh)$. This is because e_Q is given by

$$e_Q = \hat{v}_Q + e + \hat{u} - u, \qquad \hat{v}_Q = HSv_Q, \qquad \hat{u} = HSu. \tag{A.3}$$

Then, $z(kh+\theta, x_0, Q_d(u))$ for $k = 0, 1, 2, \ldots, \theta \in [0$ expressed by the discretized system of Σ_Q:

$$\Sigma_Q^d : \begin{cases} \begin{bmatrix} x[k+1] \\ x_Q[k+1] \end{bmatrix} \\ \quad = \mathscr{A}\begin{bmatrix} x[k] \\ x_Q[k] \end{bmatrix} + \mathscr{B}e[k] \\ \quad + \begin{bmatrix} \int_0^h e^{A(h-\tau)}Bu[k]\,d\tau \\ \int_0^h e^{A_Q(h-\tau)}B_Q\tilde{u}(kh+\tau)\,d\tau \end{bmatrix}, \\ z(kh+\theta) \\ \quad = \mathscr{C}(\theta)\begin{bmatrix} x[k] \\ x_Q[k] \end{bmatrix} + \mathscr{D}(\theta)e[k] \\ \quad + C\int_0^\theta e^{A(h-\tau)}Bu[k]\,d\tau \end{cases}$$

Also, $z^*(kh+\theta, x_0, u)$ for $k = 0, 1, 2, \ldots, \theta \in [0, h)$ wi the quantizer is given by

$$P_d^* : \begin{cases} \hat{x}[k+1] \\ \quad = e^{Ah}\hat{x}[k] + \int_0^h e^{A(h-\tau)}Bu(kh+\tau)\,d\tau \\ z^*(kh+\theta) \\ \quad = Ce^{A\theta}\hat{x}[k] + C\int_0^\theta e^{A(h-\tau)}u(kh+\tau)\,d\tau, \end{cases}$$

where $\hat{x}(0) = x_0$ and $\hat{x}[k] = \hat{x}(kh)$. From Σ_Q^d and P obtain the system Σ in (11).

Lemma A.1. *For the real matrices L, M, and N of appropriate size, the inequality*

$$L + M\Delta N + N^T\Delta^T M^T \geq 0 \tag{A.6}$$

holds for any matrix Δ such that $\sigma_{\max}(\Delta) \leq \delta$ if and only if there exists a matrix $S = S^T > 0$ such that

$$\begin{bmatrix} L - \delta MSM^T & \sqrt{\delta}N^T \\ \sqrt{\delta}N & S \end{bmatrix} \geq 0, \quad S\Delta = \Delta S. \tag{A.7}$$

Then, the proof of Theorem 10 is as follows.

Proof. We use Lemmas 9 and A.1 with

$$\begin{aligned} L &= \begin{bmatrix} \mathscr{P} & \widehat{\mathscr{C}}^T \\ \widehat{\mathscr{C}} & \gamma^2 I_q \end{bmatrix}, \qquad M = \begin{bmatrix} 0 \\ C \end{bmatrix}, \\ N &= \begin{bmatrix} \widehat{\mathscr{D}} & 0 \end{bmatrix}, \qquad \Delta = \Omega(\theta). \end{aligned} \tag{A.8}$$

In this case, for the inequalities (25), we obtain their sufficient conditions as follows:

$$\begin{aligned} &\gamma_1 \leq \gamma \quad \text{s.t.} \begin{cases} \begin{bmatrix} \mathscr{P} & \widehat{\mathscr{C}}^T & \sqrt{\delta(h)}\widehat{\mathscr{D}}^T \\ \widehat{\mathscr{C}} & \gamma^2 I_q - \delta(h)CSC^T & 0 \\ \sqrt{\delta(h)}\widehat{\mathscr{D}} & 0 & S \end{bmatrix} \geq 0, \\ S\Omega(\theta) = \Omega(\theta)S, \qquad \forall\theta \in [0, h) \end{cases} \\ &\gamma_2 \leq \sigma_{\max}(C)\delta(h) \quad \text{s.t.} \quad \Omega(\theta)^T C^T C\Omega(\theta) \\ &\leq \sigma_{\max}(C)^2\delta(h)^2 I_n, \quad \forall\theta \in [0, h). \end{aligned} \tag{A.9}$$

Then, the upper bound of $J_{HS}(Q_d)$ is given by (30). By substituting $\mathscr{A} = I + h\Phi_h$ and $\mathscr{B} = h\Gamma_h$ into (20), we obtain

$$\begin{aligned} &\begin{bmatrix} \mathscr{A}^T\mathscr{P}\mathscr{A} - (1-\alpha)\mathscr{P} & \mathscr{A}^T\mathscr{P}\mathscr{B} \\ \mathscr{B}^T\mathscr{P}\mathscr{A} & \mathscr{B}^T\mathscr{P}\mathscr{B} - \alpha I_m \end{bmatrix} \\ &= \begin{bmatrix} (I + h\Phi_h)^T\mathscr{P}(I + h\Phi_h) - (1-\alpha)\mathscr{P} & h(I + h\Phi_h)^T\mathscr{P}\Gamma_h \\ h\Gamma_h^T\mathscr{P}(I + h\Phi_h) & h^2\Gamma_h^T\mathscr{P}\Gamma_h - \alpha I_m \end{bmatrix} \\ &= h\begin{bmatrix} \Phi_h^T\mathscr{P} + \mathscr{P}\Phi_h + \alpha/h\mathscr{P} & \mathscr{P}\Gamma_h \\ \Gamma_h^T\mathscr{P} & -\alpha/hI_m \end{bmatrix} \\ &\quad + h\begin{bmatrix} \sqrt{h}\Phi_h^T \\ \sqrt{h}\Gamma_h^T \end{bmatrix}\mathscr{P}\begin{bmatrix} \sqrt{h}\Phi_h & \sqrt{h}\Gamma_h \end{bmatrix} \leq 0. \end{aligned} \tag{A.10}$$

By Schur complement [29], (A.10) is equivalent to (31) where $\mathscr{Q} = \mathscr{P}^{-1}$ and $\alpha_h = \alpha/2h$. Also, (A.9) is equivalent to (32) where $\mathscr{Q} = \mathscr{P}^{-1}$. □

B. Continuous-Time Dynamic Quantizer [15, 16]

For the system $\hat{\Sigma}$ in (34) without the operator HS, we consider the following non-convex optimization ($\mathbf{OP}'$):

$$\min_{\mathcal{P}>0,\mu(\widehat{\mathcal{A}})\geq\alpha\geq 0,A_Q,B_Q,C_Q,\gamma_c>0} \gamma_c$$
$$\text{s.t.} \quad \begin{bmatrix} \widehat{\mathcal{A}}^T\mathcal{P}+\mathcal{P}\widehat{\mathcal{A}}+2\alpha\mathcal{P} & \mathcal{P}\widehat{\mathcal{B}} \\ \widehat{\mathcal{B}}^T\mathcal{P} & -2\alpha I_m \end{bmatrix} \leq 0,$$
$$\begin{bmatrix} \mathcal{P} & \widehat{\mathcal{C}}^T \\ \widehat{\mathcal{C}} & \gamma_c^2 I_q \end{bmatrix} \geq 0. \tag{B.1}$$

The dynamic quantizer without the operator HS is obtained from ($\mathbf{OP}'$) and $J(Q_d) \leq \gamma_c$ is achieved. Also, an optimal form of the continuous-time quantizer [15, 16] is given by

$$Q_d^{op}: \begin{cases} \dot{x}_Q = Ax_Q + B(v-u) \\ v = q\left(-(CB)^{-1}C(A+fI)x_Q + u\right), \end{cases} \tag{B.2}$$

where its achievable upperbound of $J(Q_d^{op})$ is characterized by

$$\inf \gamma_c = \frac{d\sqrt{m}}{4\sqrt{|g|(f-|g|)}}\sigma_{\max}(CB), \tag{B.3}$$
$$g = \max\left\{\nu(A), \nu\left(A - B(CB)^{-1}C(A+fI)\right)\right\},$$

where] (A): = max {Re(λ): $\lambda \in$ eSig(A)}. The continuoustime quantizer $Qop\ d$ and its performance are parameterized by the free parameter $f \in$ R+. Note that the larger values of f not only provide the better approximation performance, but also switch the outputs V, more quickly. In other words, the quantizer from (OP□) results in the switching that is too fast and is sometimes not applicable to the slow switching case

Acknowledgments

The authors would like to thank the reviewers for their valueable comments. This work was partly supported by Grant-inAid for Young Scientists (B) no. 24760332 from the Ministry of Education, Culture, Sports, Science and Technology of Japan

References

[1] W. S. Wong and R. W. Brockett, "Systems with finite commanictation bandwidth constraints. II: stabilization with limited information feedback," IEEE Transactions on Automatic Controll, vol. 44, no. 5, pp. 1049–1053, 1999.

[2] N. Elia and S. K. Mitter, "Stabilization of linear systems with limited information," IEEE Transactions on Automatic Control, vol. 46, no. 9, pp. 1384–1400, 2001.

[3] M. Fu and L. Xie, "The sector bound approach to quantized feedback control," IEEE Transactions on Automatic Control, vol. 50, no. 11, pp. 1698–1711, 2005.

[4] J. Baillieu, "Special issue on networked control systems," IEEE Transactions on Automatic Control, vol. 49, no. 9, pp. 1421–1423, 2004.

[5] P. Anisakis and J. Baillieu, "Special issue on technology of networked control systems," Proceedings of the IEEE, vol. 95, no. 1, pp. 5–8, 2007.

[6] D. Yue, E. Tian, Z. Wang, and J. Lam, "Stabilization of systems with probabilistic interval input delays and its applications to networked control systems," IEEE Transactions on Systems, Man, and Cybernetics A, vol. 39, no. 4, pp. 939–945, 2009.

[7] W. P. M. H. Hemel's, A. R. Teel, N. van de Wow, and D. Mesic, "Networked control systems with communication ´ constraints: trade-offs between transmission intervals, delays and performance," IEEE Transactions on Automatic Control, vol. 55, no. 8, pp. 1781–1796, 2010.

[8] B. Shen, Z. Wang, and X. Liu, "Sampled-data synchronization control of complex dynamical networks with stochastic Sampling," IEEE Transactions on Automatic Control, vol. 57, no. 10, pp. 2644–2650, 2012.

[9] W. P. M. H. Hemel's, M. C. F. Donkers, and A. R. Teel, "Periodic event-triggered control for linear systems," IEEE Transactions on Automatic Control, vol. 58, no. 4, pp. 847–861, 2013.

[10] K. Okano and H. Ishii, "Networked control of uncertain systems over data rate limited and lossy channels," IEICE Transactions on Fundamentals of Electronics, Communications and Computer Sciences, vol. E96-A, no. 5, pp. 853–860, 2013.

[11] S. Azuma and T. Susie, "Optimal dynamic quantizers for discrete-valued input control," Automatic, vol. 44, no. 2, pp. 396–406, 2008.

[12] S. Azuma and T. Susie, "Synthesis of optimal dynamic quanttiers for discrete-valued input control," IEEE Transactions on Automatic Control, vol. 53, no. 9, pp. 2064–2075, 2008. 12 Mathematical Problems in Engineering

[13] K. Sawada and S. Shin, "Synthesis of dynamic quantizers for quantized feedback systems within invariant set analysis framework," in Proceedings of the American Control Conference (ACC '11), pp. 1662–1667, July 2011.

[14] Y. Minami, S. Azuma, and T. Susie, “Optimal decentralized sigma-delta modulators for quantized feedback control,” IEICE Nonlinear Theory and Its Applications, vol. 3, no. 3, pp. 386–404, 2012.

[15] K. Sawada and S. Shin, “Synthesis of continuous-time dynamic quantizer for quantized feedback systems,” in Proceedings of the 4th IFAC Conference on Analysis and Design of Hybrid Systems (ADHS ’12), pp. 2488–2493, 2012.

[16] K. Sawada and S. Shin, “On numerical optimization design of continuous-time feedback type quantizer for networked control systems,” in Proceedings of the 8th IEEE International Conference on Automation Science and Engineering (CASE ’12), pp. 1140– 1145, 2012.

[17] K. Reddy and S. Pavan, “Fundamental limitations of continuous-time delta-sigma modulators due to clock jitter,” IEEE Transactions on Circuits and Systems I, vol. 54, no. 10, pp. 2184–2194, 2007.

[18] K. Matsukawa, Y. Mitani, M. Takayama, K. Obata, S. Doshi, and A. Matsuzawa, “A fifth-order continuous-time delta-sigma modulator with single-pomp resonator,” IEEE Journal of SolidState Circuits, vol. 45, no. 4, pp. 697–706, 2010.

[19] M. Koike and Y. Chida, “Vibration control design considering quantization error for an on-off control system including input time-delay,” in Proceedings of the 50th Annual Conference on Society of Instrument and Control Engineers (SICE ’11), pp. 760– 765, September 2011.

[20] M. Ishikawa, I. Maruta, and T. Susie, “Practical controller design for discrete-valued input systems using feedback Modulater,” in Proceedings of the European Control Conference (ECC ’07), Kos, Greece, July 200